JOC Article

Synthesis of Zinc 3-Hydroxymethyl-porphyrins Possessing Carbonyl Groups at the 13- and/or 15-Positions for Models of Self-Aggregative Chlorophylls in Green Photosynthetic Bacteria

Michio Kunieda and Hitoshi Tamiaki*

Department of Bioscience and Biotechnology, Faculty of Science and Engineering, Ritsumeikan University, Kusatsu, Shiga 525-8577, Japan

tamiaki@se.ritsumei.ac.jp

Received July 1, 2008

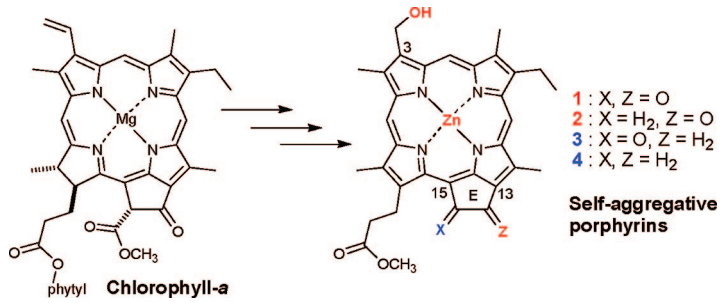

Zinc 3-hydroxymethyl-protopyropheophorbide-*d* derivatives **1**, **2**, and **3** possessing carbonyl group(s) at the 13/15-, 13-, and 15-positions, respectively, and **4** lacking the C=O group were prepared from naturally occurring chlorophyll-*a*. Zinc porphyrins **1** and **2** possessing the 13-C=O self-aggregated in an aqueous micellar solution, similarly to the self-aggregates of BChls-*c*/*d*/*e* in the main light-harvesting antenna systems of green photosynthetic bacteria, whereas **3** and **4** lacking the 13-C=O failed to make such well-ordered aggregates. These results indicated that both the presence of the C=O group and its situation at the 13-position were preferable for formation of the well-ordered *J*-aggregates.

Introduction

Self-aggregation of π-conjugated chromophores is attractive for making artificial photoactive devices, in which exciton energy is well-delocalized over the supramolecules.[1] It is well-known that metal complexes of cyclic tetrapyrroles are useful for preparation of functional supramolecules, for example, excitonically delocalized *J*-aggregates in main light-harvesting antenna systems of green photosynthetic bacteria (called chlorosomes).[2,3] Major composite molecules in chlorosomes are bacteriochlorophyll(BChl)s-*c*/*d*/*e*, which have hydroxy and carbonyl groups as well as a coordinative magnesium metal on the *y* axis (a line through N21 and N23, left drawing in Figure 1).[4−7] These three moieties are essentially required for making chlorosome-like self-aggregates based on coordination bonding (3^1-O···Mg), hydrogen bonding (3^1-O−H···O=C-13) and strong $\pi-\pi$ stacking. Many synthetic studies on clarifying the structural requirements of chlorosomal self-aggregation have been reported, and three types of π-conjugated systems, porphyrin,[8−12] chlorin,[13−22] and bacteriochlorin,[23−26] have been found acceptable for this self-aggregation. We focused on a

(1) Hoeben, F. J. M.; Jonkheijm, P.; Meijer, E. W.; Schenning, A. P. H. J. *Chem. Rev.* **2005**, *105*, 1491–1546.
(2) Blankenship, R. E.; Matsuura, K. In *Light Harvesting Antennas in Photosynthesis*; Green, B. R., Parson, W. W., Eds.; Kluwer Academic publisher: Dordrecht, 2003; pp 195−217.
(3) Olson, J. M. *Encycl. Biol. Chem.* **2004**, *2*, 325–330.
(4) Scheer, H. In *Light Harvesting Antennas in Photosynthesis*; Green, B. R., Parson, W. W., Eds.; Kluwer Academic publisher: Dordrecht, 2003; pp 29−81.
(5) Balaban, T. S.; Tamiaki, H.; Holzwarth, A. R. In *Supramolecular Dye Chemistry*; Würthner, F., Ed.; Springer: Berlin, 2005; *Top. Curr. Chem.*, Vol. 258, pp 1−38.
(6) Miyatake, T.; Tamiaki, H. *J. Photochem. Photobiol., C* **2005**, *6*, 89–107.
(7) Tamiaki, H.; Shibata, R.; Mizoguchi, T. *Photochem. Photobiol.* **2007**, *83*, 152–162.
(8) Tamiaki, H.; Kimura, S.; Kimura, T. *Tetrahedron* **2003**, *59*, 7423–7435.
(9) Balaban, T. S.; Linke-Schaetzel, M.; Bhise, A. D.; Vanthuyne, N.; Roussel, C. *Eur. J. Org. Chem.* **2004**, *391*, 9–3930.
(10) Tamiaki, H.; Kitamoto, H.; Watanabe, T.; Shibata, R. *Photochem. Photobiol.* **2005**, *81*, 170–176.
(11) Balaban, T. S.; Linke-Schaetzel, M.; Bhise, A. D.; Vanthuyne, N.; Roussel, C.; Anson, C. E.; Buth, G.; Eichhoefer, A.; Foster, K.; Garab, G.; Gliemann, H.; Goddard, R.; Javorfi, T.; Powell, A. K.; Roesner, H.; Schimmel, T. *Chem. Eur. J.* **2005**, *11*, 2267–2275.
(12) Ptaszek, M.; Yao, Z.; Savithri, D.; Boyle, P. D.; Lindsey, J. S. *Tetrahedron* **2007**, *63*, 12629–12638.
(13) Tamiaki, H.; Amakawa, M.; Shimono, Y.; Tanikaga, R.; Holzwarth, A. R.; Schaffner, K. *Photochem. Photobiol.* **1996**, *63*, 92–99.

10.1021/jo8014402 CCC: $40.75
Published on Web 08/27/2008

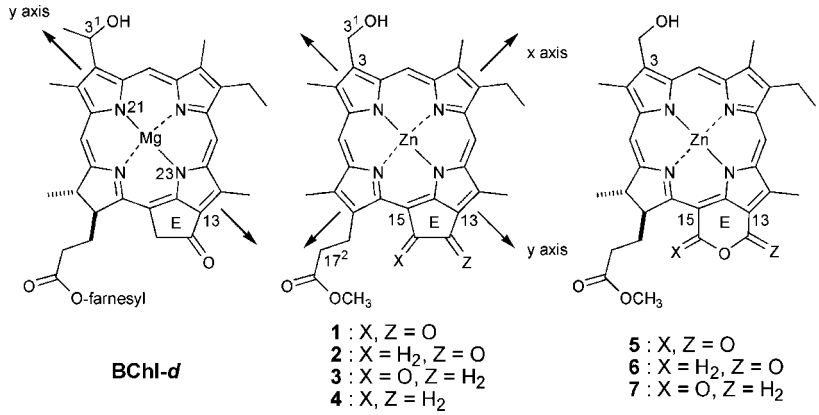

FIGURE 1. Molecular structures of a natural BChl-*d* (left), chlorosomal model porphyrins **1**−**4** (center), and chlorins **5**−**7** (right).

SCHEME 1. Synthesis of Zinc 3-Hydroxymethyl-13,15-dicarbonyl-porphyrin 1[a]

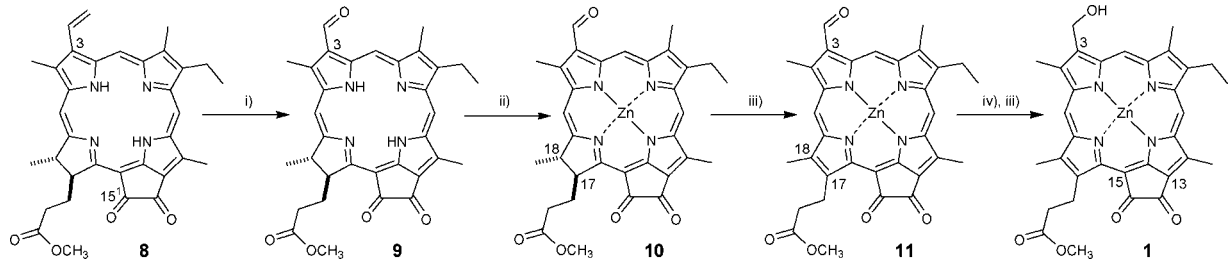

[a] Reagents and conditions: (i) cat. OsO_4, $NaIO_4$, THF−1,4-dioxane−water; (ii) $Zn(OAc)_2 \cdot 2H_2O$, CH_2Cl_2−methanol; (iii) DDQ, acetone; (iv) tBuNH$_2 \cdot$BH$_3$, CH_2Cl_2.

porphyrin π-system in this report, because the fully conjugated π-system is significantly stable, and the intense Soret band of the aggregated porphyrin situated at around 400−550 nm is well-matched with the sunlight spectrum.

Recently we reported that zinc 3-hydroxymethyl-purprin 18 derivative **5** (right in Figure 1) possessing acid anhydride moiety on the exo six-membered ring instead of the natural exo five-membered E-ring formed chlorosomal self-aggregates in aqueous media, similarly to natural BChls and synthetic models.[27] Furthermore, we have examined self-aggregation behaviors of its monodecarbonylated chlorins **6** and **7** possessing a six-membered lactone E-ring (right in Figure 1) in a nonpolar organic solvent: **6** possessing 13-C═O self-aggregated, whereas **7** possessing 15-C═O remained monomeric.[28]

We designed four porphyrins, zinc 3-hydroxymethyl-protopyropheophorbide-*d* derivatives **1**−**4** (see molecular structures in center of Figure 1) to clarify the structural requirements for chlorosomal self-aggregation. Zinc porphyrin **2** possessing a C═O group at the 13-position was previously reported[10] and self-aggregated to form a large oligomer (*J*-aggregates) possessing a supramolecule similar to the chlorosomal. The others are novel synthetic zinc porphyrins **1**, **3**, and **4**, of which the first have two C═O groups at the 13- and 15-positions, the second has one C═O at the 15-position, and the third has no C═O on the E-ring. These porphyrins **1**−**3** are distinguished from the previous purpurin derivatives **5**−**7** by the presence of a keto-carbonyl group on the five-membered ring and their fully conjugated porphyrin π-system. Here we report synthesis of zinc porphyrins **1**−**4** and their self-aggregation behaviors in an aqueous Triton X-100 (TX-100) solution.

Results and Discussion

Synthesis of Zinc 3-Hydroxymethyl-porphyrins 1−4. Zinc 3-hydroxymethyl-13,15-dicarbonyl-porphyrin **1** was synthesized from methyl 15[1]-oxo-pyropheophorbide-*a* (**8**)[29] according to Scheme 1. Oxidative cleavage of the 3-vinyl group[13] in **8** gave 3-formyl-chlorin **9** in 70% yield. After metalation[13] of **9** to zinc complex **10** (96%), the skeletal chlorin π-system (C17−C18) was converted to the porphyrin π-system (C17═C18) by treatment of 2,3-dichloro-5,6-dicyanobenzoquinone (DDQ),[10] affording zinc 3-formyl-dioxoporphyrin **11** (90%). Zinc porphyrin **11** had one aldehyde (3-CHO) and two keto-carbonyl groups (13- and 15-C═O), all of which had potential to react with a reductant. Treatment of **11** by tBuNH$_2 \cdot$BH$_3$ complex[13] gave a mixture of products that were easily separated by normal-phase HPLC, affording four compounds (see Chart 1) in the

(14) Huber, V.; Katterle, M.; Lysetska, M.; Wuerthner, F. *Angew. Chem., Int. Ed.* **2005**, *44*, 3147–3151.
(15) Kunieda, M.; Tamiaki, H. *Eur. J. Org. Chem.* **2006**, *235*, 2–2361.
(16) Katterle, M.; Prokhorenko, V. I.; Holzwarth, A. R.; Jesorka, A. *Chem. Phys. Lett.* **2007**, *447*, 284–288.
(17) Tamiaki, H.; Watanabe, T.; Kunieda, M. *Res. Chem. Intermed.* **2007**, *33*, 161–168.
(18) Shibata, R.; Mizoguchi, T.; Inazu, T.; Tamiaki, H. *Photochem. Photobiol. Sci.* **2007**, *6*, 749–757.
(19) Tamiaki, H.; Nishiyama, T.; Shibata, R. *Bioorg. Med. Chem. Lett.* **2007**, *17*, 1920–1923.
(20) Mizoguchi, T.; Tamiaki, H. *Bull. Chem. Soc. Jpn.* **2007**, *80*, 2196–2202.
(21) Shibata, R.; Koike, K.; Hori, H.; Tamiaki, H. *Chem. Lett.* **2008**, *37*, 532–533.
(22) Zupcanova, A.; Arellano, J. B.; Bina, D.; Kopecky, J.; Psencik, J.; Vacha, F. *Photochem. Photobiol.* **2008**, Epub ahead of print; DOI 10.1111/j.1751-1097.2008.00312x.
(23) Kunieda, M.; Mizoguchi, T.; Tamiaki, H. *Photochem. Photobiol.* **2004**, *79*, 55–61.
(24) Kunieda, M.; Tamiaki, H. *J. Org. Chem.* **2005**, *70*, 820–828.
(25) Sasaki, S.-i.; Tamiaki, H. *J. Org. Chem.* **2006**, *71*, 2648–2654.
(26) Kunieda, M.; Yamamoto, K.; Sasaki, S.-i.; Tamiaki, H. *Chem. Lett.* **2007**, *36*, 936–937.
(27) Tamiaki, H.; Shimamura, Y.; Yoshimura, H.; Pandey, S. K.; Pandey, R. K. *Chem. Lett.* **2005**, *34*, 1344–1345.
(28) Tamiaki, H.; Yoshimura, H.; Shimamura, Y.; Kunieda, M. *Photosynth. Res.* **2008**, *95*, 223–228.
(29) Rosenfeld, A.; Morgan, J.; Goswami, L. N.; Ohulchanskyy, T.; Zheng, X.; Prasad, P. N.; Oseroff, A.; Pandey, R. K. *Photochem. Photobiol.* **2006**, *82*, 626–634.

CHART 1. Reduction of Zinc 3,13,15-Tricarbonyl-porphyrin 11

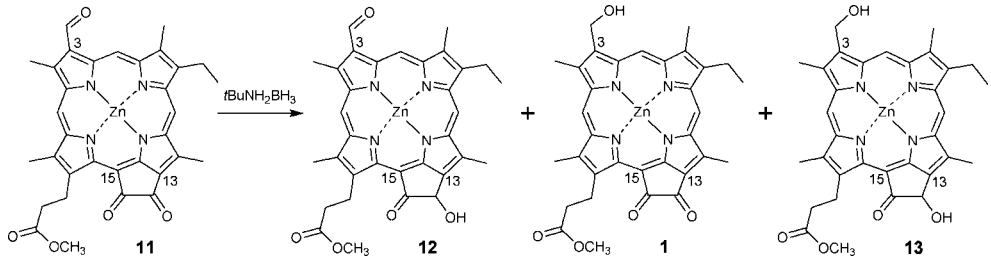

SCHEME 2. Synthesis of Zinc 3-Hydroxymethyl-15-carbonyl-porphyrin 3 and Its 15-Decarbonylated Compound 4[a]

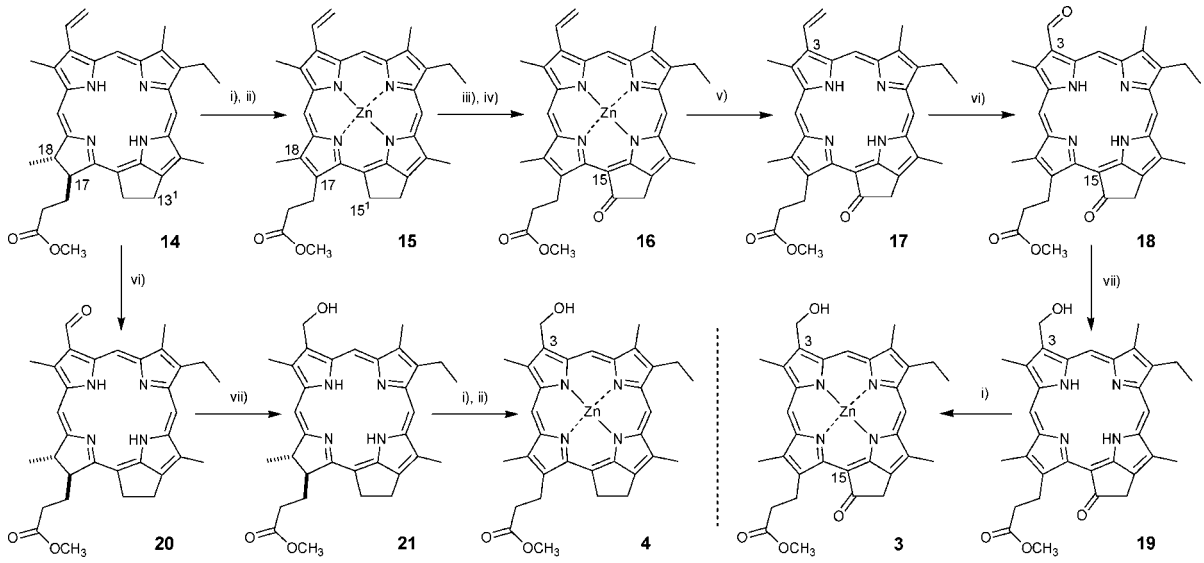

[a] Reagents and conditions: (i) $Zn(OAc)_2 \cdot 2H_2O$, CH_2Cl_2−methanol; (ii) DDQ, acetone; (iii) Al_2O_3, CH_2Cl_2−methanol; (iv) nPr_4NRuO_4, *N*-methylmorpholine *N*-oxide, CH_2Cl_2; (v) aq 10% HCl, CH_2Cl_2; (vi) cat. OsO_4, $NaIO_4$, THF−1,4-dioxane−water; (vii) $tBuNH_2 \cdot BH_3$, CH_2Cl_2.

eluted order of unreacted **11** (16%), 13-reduced **12** (30%, 3-CHO/13-CHOH/15-C═O), desired 3-reduced **1** (26%, 3-CH_2OH/13,15-C═O), and 3,13-reduced **13** (19%, 3-CH_2OH/13-CHOH/15-C═O). One of the reasons the 15-C═O was not reduced is the steric effect of a neighboring large propionate side chain at the 17-position. Generally a keto-carbonyl group such as the 13-C═O of chlorins or porphyrins could be reduced by slightly strong reductants ($NaBH_4$, $LiAlH_4$, etc.) but not by mild reductants like $tBuNH_2 \cdot BH_3$. Electronically coupled 13- and 15-C═O groups in α,β-dioxo-form **11** affected each other so that they became more reactive upon the reduction, but the sterically less crowded 13-C═O was reduced more rapidly than the neighboring 15-C═O. The absence of the electronic coupling in the predominantly 13-reduced product **12** led the 15-C═O to be less reactive and was not further reduced. The low yield of **1** was improved by the following successive procedures: complete reduction of **11** to **13** followed by reoxidation of **13** to **1** [steps (iv) and (iii) of Scheme 1]. Treatment of **11** by a slightly excess amount of $tBuNH_2 \cdot BH_3$ with prolonged stirring resulted in the sole formation of **13** (not isolated but confirmed by ^1H NMR). The crude **13** was treated by DDQ to afford pure **1** (78% from **11**) after FCC purification, in which the primary alcohol (3-CH_2OH) in **13** was not oxidized by DDQ. Zinc 3-hydroxymethyl-13-carbonyl-porphyrin **2** was prepared by reported procedures.[10]

Synthesis of zinc 3-hydroxymethyl-15-carbonyl-porphyrin **3** was achieved as follows (Scheme 2). The chlorin π-system in methyl 13^1-deoxo-pyropheophorbide-*a* (**14**)[30] was converted to a porphyrin π-system (vide supra) to give zinc porphyrin **15** (67%). The resulting **15** was oxidized on aluminum oxide to give 15^1-hydroxy-porphyrin (not isolated).[31] After oxidation of the 15^1-hydroxy to 15^1-oxo group (15-C═O) by combination of nPr_4NRuO_4 with *N*-methylmorpholine *N*-oxide,[32] FCC purification gave 15-carbonylated porphyrin **16** (44% from **15**). The central zinc atom in **16** was removed by an action of HCl[33] to give **17** (95%), whose 3-vinyl group was converted to the 3-fromyl group, affording 3-formyl-15-keto-porphyrin **18** (69%). Under such oxidative conditions, zinc porphyrin was so unstable that the central metal was preliminarily removed. After reduction of the 3-formyl group in **18** to 3-hydroxymethyl-porphyrin **19** (89%), remetalation of **19** afforded desired zinc 3-hydroxymethyl-15-carbonyl-porphyrin **3** (88%). Zinc 3-hydroxymethyl-porphyrin **4** lacking any keto-carbonyl group on the E-ring was synthesized from **14** in synthetic procedures similar to those described above [**14** → **20**[34] (67%), **20** → **21** (89%), and **21** → **4** (72%)]. Molecular structures of all the compounds were

(30) Tamiaki, H.; Yagai, S.; Miyatake, T. *Bioorg. Med. Chem.* **1998**, *6*, 2171–2178.

(31) A similar oxidation of CH_2 to C═O in a synthetic chlorin by an aluminum oxide has been reported: Taniguchi, M.; Kim, H.-J.; Ra, D.; Schwartz, J. K.; Kirmaier, C.; Hindin, E.; Diers, J. R.; Prathapan, S.; Bocian, D. F.; Holten, D.; Lindsey, J. S. *J. Org. Chem.* **2002**, *67*, 7329–7342.

(32) Kunieda, M.; Tamiaki, H. *J. Org. Chem.* **2007**, *72*, 2443–2451.

(33) Tamiaki, H.; Takeuchi, S.; Tsudzuki, S.; Miyatake, T.; Tanikaga, R. *Tetrahedron* **1998**, *54*, 6699–6718.

(34) Wiederrecht, G. P.; Svec, W. A.; Niemczyk, M. P.; Wasielewski, M. R. *J. Phys. Chem.* **1995**, *99*, 8918–26.

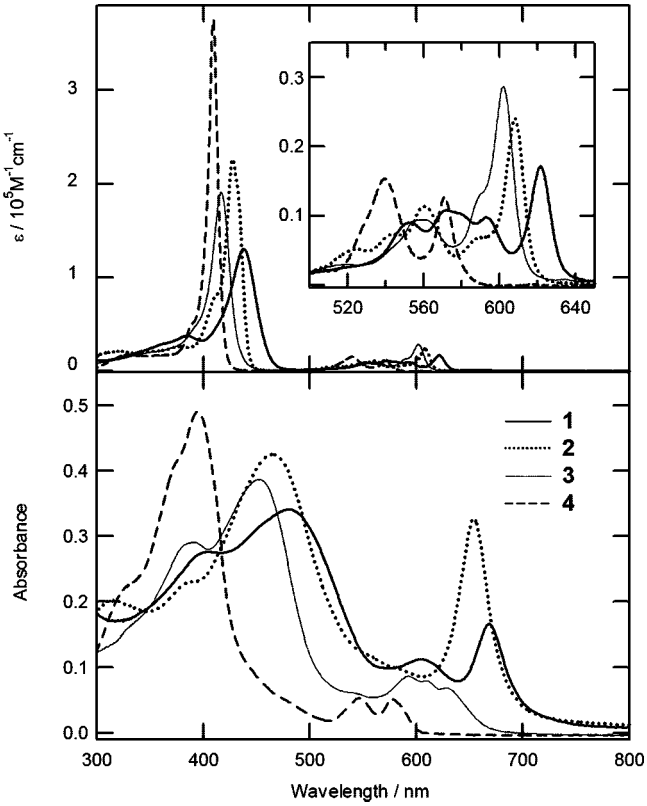

FIGURE 2. UV−vis spectra of zinc porphyrins **1**−**4** in THF (upper) and aqueous 0.025 % v/v TX-100 solution containing 1.0 % v/v DMSO (lower). Bold, dotted, thin, and broken lines are for **1**, **2**, **3**, and **4**, respectively. Concentrations of samples in lower graph were 10 μM.

determined by their ^{1}H and ^{1}H−^{1}H COSY/NOESY NMR and FAB-MS spectra.

Monomeric Zinc Porphyrins 1−4 in THF. UV−vis Spectroscopy. The present zinc porphyrins **1**−**4** had the same peripheral substituent groups, except for the number and situation of the oxo group on the E-ring. In UV−vis spectroscopy, each THF solution of zinc porphyrins **1**−**4** showed intense Soret (combination of Bx and By transitions) and relatively small Q bands (Qx and Qy transitions) at around 400−440 and 520−640 nm, respectively, which were characteristic of monomeric zinc porphyrins.[9,10,35] UV−vis spectrum of zinc porphyrin **4** lacking any C═O group on the E-ring in THF (broken line in Figure 2 upper graph) showed a sharp Soret absorption band at 409 nm, which indicated that its almost equivalent Bx and By transitions were situated at almost the same wavelength to produce the sharp band: the full width at half-maximum (fwhm) was 630 cm^{-1} (Table 1). The molar coefficient of **4** in THF was 370,000 M^{-1} cm^{-1} at the Soret band. Two Q bands appeared at 540 and 571 nm, which were well-separated and could be tentatively assigned as Qx and Qy transitions from blue to red. These characters were similar to those of the fully synthesized zinc porphyrins having no C═O group (C4 symmetrical *meso*-tetraphenylporphyrin[36] and β-octaethylporphyrin[35]), indicating that π-conjugated system of **4** lacking any C═O group on the E-ring would be nearly pseudo-C4 symmetry despite the presence of the E-ring.[35]

(35) Kunieda, M.; Nakato, E.; Tamiaki, H. *J. Photochem. Photobiol., A* **2007**, *185*, 321–330.

(36) Tamiaki, H.; Matsumoto, N.; Unno, S.; Shinoda, S.; Tsukube, H. *Inorg. Chim. Acta* **2000**, *300*−*302*, 243–249.

TABLE 1. Absorption Maxima of 1−4 in THF and Aqueous 0.025 % v/v TX-100 Solutions Containing 1.0 % v/v DMSO, and Their Red-Shift Values of the Redmost Qy Band by Self-Aggregation

	absorption maxima, nm					
	Soret		redmost Qy		Δ, cm^{-1}	
compound	monomer[a]	aggregate	monomer	aggregate	Soret	Qy
1	438 (1630)	489	621	671	2380	1200
2	427 (1000)	465	608	655	1910	1180
3	417 (1120)	451	602	629	1810	710
4	409 (1630)	395	571	578		

[a] Values in parenthesis indicate fwhm's (cm^{-1}).

The UV−vis spectra of zinc porphyrins **1**−**3** possessing oxo group(s) on the E-ring were clearly distinguished from that of **4**. Compared to the absorption maxima of **4**, the presence of the 15-C═O, 13-C═O, and 13/15-C═O caused red-shifts in their absorption maxima in this order (Figure 2 upper and Table 1). Such red-shifts in the absorption maxima of **1**−**3** were explained by the electron-withdrawing effect of C═O group(s) conjugated to the macrocyclic π-system.[35] UV−vis spectra of zinc porphyrins **2** and **3** possessing one C═O group at the 13- and 15-positions, respectively (in THF, dotted and thin lines in Figure 2 upper, Table 1), showed their Soret absorption maxima at 427 and 417 nm with fwhm's of 1000 and 1120 cm^{-1}. Their molar coefficients at the Soret band were 230,000 and 190,000 M^{-1} cm^{-1} for **2** and **3**, respectively, both of which were smaller than that of **4**. The red-shifts were due to the electron-withdrawing effect of C═O group (vide supra), and their broader Soret bands and lower molar coefficients were ascribable to symmetry breaking of the porphyrin π-system by the conjugation of the C═O: Bx and By transition components in a Soret region should have different energy levels to be wider Soret bands.

The Q bands of **2** and **3** in THF were also affected by the conjugation of C═O group. There were two Q bands at around 550−570 (Qx) and 600−610 nm (Qy), both of which showed asymmetrical spectral shapes, compared to **4** (inset in Figure 2 upper). Symmetry breaking by a conjugation of C═O would generate distinct vibrational bands for each Q-band, i.e., (0,1) and/or (0,2) transitions. Between the two regioisomers 13-C═O-**2** and 15-C═O-**3**, a spectral difference was clearly observed. Major Soret and redmost Qy absorption bands of **2** were shifted to wavelengths longer than those of **3**, which was due to the different situation of the conjugated C═O group on the E-ring: the 13-C═O group in **2** was on the Qy transition dipole moment of the molecule (see center drawing in Figure 1), whereas the 15-C═O group in **3** was out of the *y*-axis.

UV−vis spectrum of **1** possessing two C═O groups at the 13- and 15-positions in THF showed the most red-shifted Soret and Q bands (bold line in Figure 2 upper, Table 1). The co-presence of two C═O groups at the 13- and 15-positions caused such red-shifts and broadened Soret band (fwhm of 1630 cm^{-1}). The molar coefficient at the Soret band of **1** in THF was 130,000 M^{-1} cm^{-1} and was the smallest value among the present porphyrins. This broadening was ascribable to the large splitting between Bx and By transitions, which might be induced by the presence of the two C═O groups. Q bands of 13/15-C═O-**1** in THF were further split, compared to those of **2** and **3** possessing one C═O group on the E-ring, affording four or five bands, of which the energetically lowest band at 621 nm can be assigned as Qy(0,0) transition.

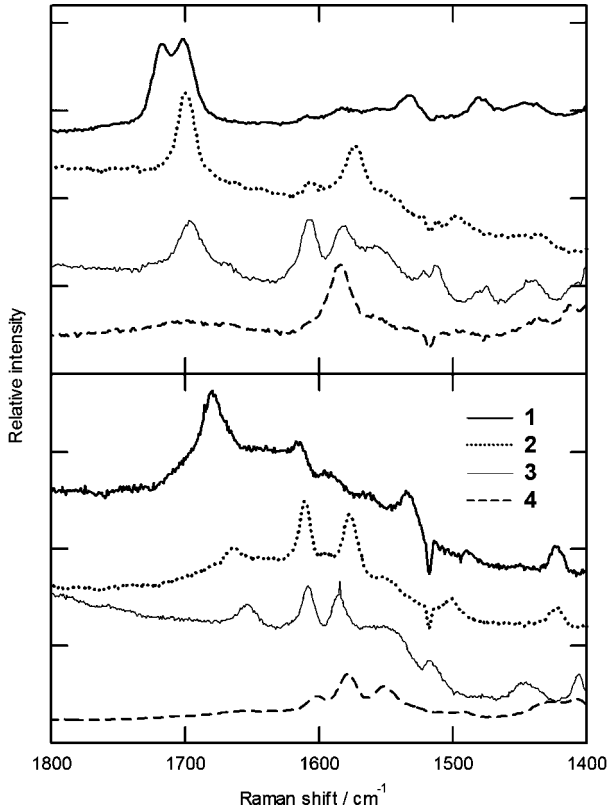

FIGURE 3. RR spectra of zinc porphyrins **1**−**4** in THF (upper) and aqueous 0.025 % v/v TX-100 solution containing 1.0 % v/v DMSO (lower). Bold, dotted, thin, and broken lines represent **1**, **2**, **3**, and **4**, respectively. Concentrations of all samples in the lower graph were 10/10/50/50 μM for **1/2/3/4**, and their UV−vis spectral shapes were the same as those in Figure 2 lower. Aqueous TX-100 solutions of zinc porphyrins **1**−**3** were excited by a 488-nm laser, and the others (including monomer in THF solution) were excited at 405 nm.

Resonance Raman (RR) and FT-IR Spectroscopies. RR spectra of zinc porphyrins **1**−**4** in THF excited at 405 nm showed some vibrational signals corresponding to their skeletal C−C, C═C, C−N, C═N stretchings and bendings in the region below 1640 cm^{-1} (Figure 3 upper). The vibrational signal of the 17^2-C═O group in all of the porphyrins was less active in the RR spectroscopy due to there being no conjugation of the 17^2-C═O group with the π-system absorbing 405-nm light, but it could be observed on their FT-IR spectra in 1 % v/v pyridine–THF: all of the 17^2-C═O were situated at 1739 cm^{-1} (see Figure S1 upper in Supporting Information). Zinc porphyrins **1**−**3** having C═O group(s) on the E-ring gave intense Raman shifts at around 1700 cm^{-1}, which were ascribable to the C═O stretchings conjugated with the π-system as compared with the previous reports.[13,37] Raman shifts of 13- and 15-C═O vibrational signals in **2** and **3** were observed at 1699 and 1695 cm^{-1}, respectively (dotted and thin lines in Figure 3 upper). Zinc porphyrin **1** possessing two 13- and 15-C═O groups showed two signals at 1701 and 1718 cm^{-1} (bold line in Figure 3 upper), both of which were also observed on the FT-IR spectrum (Figure S1). As a result of the coupling between 13- and 15-C═O groups in **1**, the RR signal of monomer **1** in the solution was not reproduced with the simple combination of two peaks in **2** and **3**. RR spectrum of zinc porphyrin **4** lacking any C═O group showed no signal at around 1700 cm^{-1} as expected (broken line in Figure 3 upper).

Zinc Porphyrins 1−4 in an Aqueous TX-100 Solution. When a DMSO solution[38] of zinc porphyrins **1**−**4** containing an appropriate amount of TX-100 (0.025 % v/v) was diluted with water (the final concentrations of **1**−**4** were 10 μM), their UV−vis (Figure 2 lower) and RR spectra (Figure 3 lower) showed significant changes, compared with their monomeric spectra (Figures 2 and 3 upper). Usually, the hydrophobic environments inside aqueous micelles are suitable for creating intermolecular interactions among π-conjugated dyes, such as coordination and hydrogen-bonding found in chlorosomal self-aggregates.[15,32,39] We discuss the self-aggregation behaviors of the present zinc porphyrins **1**−**4** in the above microheterogeneous medium, which is divided in cases of the presence and absence of the 13-C═O on the E-ring. First, we discuss the optical properties of zinc porphyrins **1** and **2** possessing the 13-C═O group.

Self-Aggregation of Zinc Porphyrins 1 and 2 Possessing 13-C═O in Aqueous TX-100 Solution. UV−vis Spectroscopy. The UV−vis spectrum of 13-C═O-**2** (dotted line in Figure 2 lower) showed broadened and red-shifted absorption bands in the aqueous solution, which was the same behavior as the self-aggregation of the previous report (**2** in nonpolar organic and aqueous TX-100 solution).[10,40] The absorption maxima of Soret and Qy bands in the self-aggregated **2** were situated at 465 and 655 nm, respectively, which were red-shifted by 1910 and 1180 cm^{-1} from those of monomer **2** in THF (Table 1). A small shoulder peak at around 560 nm might be induced from the Qx transition. These indicated that 13-C═O-**2** self-aggregated in the aqueous micellar solution to make chlorosomal *J*-aggregates, similar to the self-aggregation of natural and synthetic chlorosomal chlorophylls.[6,8−11,14,15,21,27,28,32,41]

Similar spectral changes were observed for 13/15-C═O-**1** in aqueous 0.025 % v/v TX-100 solution (bold line in Figure 2 lower, Table 1). The absorption maxima of the Soret and Qy bands of **1** in the aqueous solution were situated at 489 and 671 nm, respectively, which were red-shifted from monomeric **1** in THF solution (438 and 621 nm). The red-shift values of Soret and Qy bands by self-aggregation of **1** (2380 and 1200 cm^{-1}) were comparable to those in self-aggregation of **2**. The absorption maxima of self-aggregated **1** moved to a longer wavelength region than those of self-aggregated **2**, which was an obvious reflection of the red-shifted Soret and Qy bands in the monomeric states (ca. 10 nm for **2** → **1**, see Table 1). The largely broadened Soret band in the self-aggregated **1** was also ascribable to the monomeric broadened Soret band (1.6 fold increase in fwhm's, 1000 → 1630 cm^{-1}). A small and broadened band at around 600 nm in the self-aggregated **1** would be due to the Qx transition, as also observed in **2**.

RR and FT-IR Spectroscopies. RR spectrum of 13-C═O-**2** in the TX-100 solution (dotted line in Figure 3 lower) showed disappearance of a peak at 1699 cm^{-1} assigned to the monomeric 13-C═O stretching, and the appearance of a new peak at

(37) Morishita, H.; Tamiaki, H. *Tetrahedron* **2005**, *61*, 6097–6107.

(38) An aqueous TX-100 solution containing self-aggregates of zinc porphyrin was also prepared by dilution of the THF solution with water. However, the solubility of the present zinc porphyrin, especially 13/15-C═O-**1** in THF was so low that DMSO was used as an alternative monomerized solvent.

(39) Miyatake, T.; Tamiaki, H.; Holzwarth, A. R.; Schaffner, K. *Helv. Chim. Acta* **1999**, *82*, 797–810.

(40) Tamiaki, H.; Sumi, H. In *Photosynthesis. Energy from the Sun: 14th International Congress on Photosynthesis Research 2007*; Allen, J. F., Gantt, E., Golbeck, J. H., Osmond, B., Eds.; Springer, Heidelberg: 2008, pp 329−331.

(41) Balaban, T. S. *Acc. Chem. Res.* **2005**, *38*, 612–623.

1663 cm^{-1}. This spectral change was fairly consistent with those of the previously synthesized cyclic tetrapyrroles:[10,13,42] the down-shifted peak at 1663 cm^{-1} was assigned to the vibrational stretching signal of the 13-C═O group bonded to 3^1-OH group in another porphyrin. Similar spectral change was obtained by FT-IR spectrum of the thin film of **2** (Figure S1 lower). Many reports confirmed that chlorosomal chlorophyllous pigments self-aggregated in a solid state, whose spectral features were nearly the same as *J*-aggregates in a solution state.[10,13,24,42−44] In addition to the down-shifted 13-C═O (1698 → 1659 cm^{-1}), FT-IR spectrum of **2** in the solid state showed the 17^2-C═O vibrational signal, which did not show such a significant change (1739 → 1735 cm^{-1}).

RR spectrum of 13/15-C═O-**1** (bold line in Figure 3 lower) also showed disappearance of its monomeric C═O stretchings (1701/1718 cm^{-1}) and appearance of a new peak (1680 cm^{-1}), which were consistent with the FT-IR spectral change (Figure S1). The disappearance of both the 1701 and 1718 cm^{-1} peaks was explained in two ways: (i) both the 13- and 15-C═O groups bonded with hydroxy groups of another porphyrin or water molecule; (ii) one of the two C═O groups intermolecularly hydrogen-bonded with the 3^1-OH group in the self-aggregates and the resulting hydrogen-bonded C═O affected the neighboring C═O stretching. Compared with the 15-C═O group near a large 17-propionate side chain, the 13-C═O group is sterically less hindered so that it can be more interactive with the hydrogen-bond intermolecularly. As observed in the previously reported purprin derivative **5** (Figure 1),[28] chlorosomal pigments possessing two C═O groups on the E-ring self-aggregated to form *J*-aggregates, indicating that the additional C═O group did not disturb the self-aggregation.

Zinc Porphyrins 3 and 4 lacking 13-C═O in Aqueous TX-100 Solution. UV−vis Spectroscopy. Red-shifts of 1000−2000 cm^{-1} and broadening for the Soret and Qy bands are characteristic of chlorosomal *J*-aggregation of zinc porphyrins **1** and **2**, as well as natural chlorosomal BChls and the previous models as described above. In contrast, the aqueous micellar solution of 15-C═O-**3** possessing the chlorosomal substituents (OH, Zn and C═O) in a nonlinear order (the angle of $C3^1$−Zn−C15 was 151° in an energetically minimized molecular structure obtained by MM+/PM3 calculations,[15] and that of $C3^1$−Zn−C13 in **2** was 170°) gave a different UV−vis spectrum (thin line in Figure 2 lower). The Soret absorption band of **3** in the aqueous solution moved to a longer wavelength region, similar to chlorosomal *J*-aggregations of **1** and **2**, while three peaks apparently appeared at 597, 610 and 629 nm in a Qy region. The split bands might indicate the presence of three species, monomer, dimer, and oligomer. This possibility was easily ruled out, however, because an intense Soret absorption peak of monomer situated at around 420 nm had completely disappeared. Furthermore, the UV−vis spectrum at a 10-times higher concentration (ca. 100 μM) in an aqueous TX-100 solution showed the same spectrum having the three peaks as that of [**3**] = 10 μM, indicating that the spectra were independent of the concentration. The three bands were not due to the presence of several species and would arise from one oligomeric species; for example, the three bands could be assigned to Qy(0,0), Qy(0,1) and Qx(0,0) from red to blue.

The red-shift value of the redmost Qy band by self-aggregation of **3** (602 → 629 nm) was 710 cm^{-1}, which was smaller than those of **1** and **2**. The relative intensity of the redmost band for self-aggregated **3** was obviously smaller than those of **1** and **2**. These indicated that 15-C═O-**3** self-aggregated to form slipped overlapping *J*-aggregates (confirmed by largely red-shifted and broadened Soret band) inside a micelle, but the transition dipole moments of the composite molecules (especially Qy transition) would be disordered in the supramolecular structure due to the nonlinear order of OH, Zn and C═O. In a previous report,[28] zinc chlorin **6** possessing 13-C═O self-aggregated similarly to the chlorosomal BChls while **7** possessing 15-C═O failed to form such chlorosomal *J*-aggregates. A major difference between the previous and present studies is the skeletal π-system of the composite molecule: $\pi-\pi$ stacking among the fully conjugated and more planar porphyrin π-system as in **3** should be stronger than that in chlorin **7**. Thus zinc porphyrin **3** would form *J*-aggregates in spite of lacking 13-C═O group, but the supramolecular structure was more amorphous than the chlorosomal.

The role of the 15-C═O group in **3** in the formation of *J*-aggregates was confirmed by UV−vis spectral change of **4** lacking any C═O groups (broken line in Figure 2 lower). UV−vis spectrum of **4** in the aqueous solution showed broadened absorption bands but the absorption maxima were shifted to a lesser degree (Table 1). The Soret band of **4** in the solution was shifted to a shorter wavelength region with its broadening, while the redmost Qy band of **4** in the solution was slightly red-shifted. Some intermolecular interaction, coordination bonding between 3^1-OH and Zn, and π-π stacking among the molecules might occur in **4** but these were not enough to make large *J*-aggregates, in contrast to zinc porphyrin **3** possessing 15-C═O group. For *J*-aggregation of natural chlorophyll derivatives, at least one C═O group on the E-ring as well as the presence of OH and coordinative metal are necessary, and this group's situation in the molecular structure is preferably on the *y*-axis to make transition dipole moments well-ordered in the supramolecular structure of chlorosomal *J*-aggregates.

RR and FT-IR Spectroscopies. RR spectra of **3** and **4** were measured in an aqueous TX-100 solution. The RR spectra of **4** lacking any C═O group on the E-ring is not further discussed in this section because it showed less difference than that of monomeric **4** in THF (vide supra).

The Raman shift of 15-C═O in **3** moved to a lower wavenumber from its monomer in THF to oligomer in the aqueous TX-100 solution (thin line in Figure 3). The down-shift value of 42 cm^{-1} (1695 → 1653 cm^{-1} from monomer to aggregate) was comparable to those of **1** (1718/1701 → 1680 cm^{-1}) and **2** (1699 → 1663 cm^{-1}), indicating that the 15-C═O group in **3** played an important role in the intermolecular interaction for making its *J*-aggregates. Such a down-shift was also observed on the FT-IR spectral analysis (Figure S1). There are two possible explanations for this down-shift: one is coordination bonding (15-C═O···Zn),[11] and the other is hydrogen-bonding among molecules of **3** (15-C═O···H−O-3^1) or a molecule of **3** with a water molecule (15-C═O···H−OH). The 15-C═O group is conformationally fixed on the E-ring to be coplanar with the porphyrin π-system and the presence of the neighboring 17-propionate side chain would disturb the former coordination. To clarify the down-shift of

(42) Mizoguchi, T.; Shoji, A.; Kunieda, M.; Miyashita, H.; Tsuchiya, T.; Mimuro, M.; Tamiaki, H. *Photochem. Photobiol. Sci.* **2006**, *5*, 291–299.
(43) Tamiaki, H.; Amakawa, M.; Holzwarth, A. R.; Schaffner, K. *Photosynth. Res.* **2002**, *71*, 59–67.
(44) Kunieda, M.; Mikata, Y.; Tamiaki, H. *J. Org. Chem.* **2007**, *72*, 7398–7401.

the 15-C═O in aqueous TX-100 solution of **3**, we measured UV−vis and RR spectra of zinc 2-vinyl-15-carbonyl-porphyrin **16** (see Scheme 2) lacking 3^1-OH in an aqueous TX-100 solution. As compared to a THF solution of **16**, slightly red-shifted Qy and broadened Soret bands (Figure S2A) and a slightly down-shifted RR peak (1692 → 1688 cm^{-1}, Figure S2B) were observed, clearly showing that both the coordination of Zn with 15-C═O and hydrogen-bonding of 15-C═O with a water molecule did not occur in the micellar solution. These results indicated that the presence of 3^1-OH was needed for *J*-aggregation and the down-shift of the 15-C═O observed in aqueous TX-100 solution of **3** should be due to hydrogen-bonding between 3^1-OH and 15-C═O. Therefore, it is assumed that zinc porphyrin **3** could *J*-aggregate by use of hydrogen-bonding between 15-C═O and 3^1-OH groups. Due to the absence of the 13-C═O group, zinc porphyrin **3** alternatively used the 15-C═O group as the hydrogen-bonding acceptor for the self-aggregation, but the bent alignments of the OH, Zn and C═O moieties in **3** resulted in the disordered Qy transition dipole moments in the *J*-aggregates.

Conclusions

Zinc 3-hydroxymethyl-porphyrins **1** and **2** possessing an oxo group at the 13^1-position self-aggregated in an aqueous TX-100 solution, similarly to the natural chlorosomal BChls and their synthetic models having 13-C═O, whereas **3** and **4** lacking the 13^1-oxo group gave different species. Zinc porphyrin **4** lacking any oxo group on the E-ring failed to achieve chlorosomal self-aggregation because of the absence of hydrogen-bonding acceptor (13-C═O) in a molecule. An aqueous TX-100 solution of zinc porphyrin **3** possessing the 15-C═O group showed a red-shifted Soret absorption band, characteristic of *J*-aggregation. However, the less red-shifted and smaller Qy(0,0) band in the self-aggregates suggested that the transition dipole moments of the composite molecules in the *J*-aggregates were disordered due to the nonlinear order of the OH, Zn and C═O in a molecule. Since stacking ability of a planar porphyrin π-system is stronger than that of a chlorin π-system, zinc porphyrin **3** stacked to form *J*-aggregates, in sharp contrast to the previously reported 15-C═O chlorin **7**, which gave no self-aggregates.

Experimental Section

Synthetic Compounds. Methyl 15^1-Oxo-pyropheophorbide-*d* (9). To a THF (40 mL) and 1,4-dioxane (5 mL) solution of **8**[29] (120.2 mg, 0.21 mmol) was added a catalytic amount of OsO_4 (ca. 5 mg, ca. 20 μmol), and the mixture was stirred under nitrogen. After 5 min of stirring, an aqueous solution (4 mL) of $NaIO_4$ (605 mg, 0.36 mmol) was added, and the mixture was stirred for 4 h under nitrogen. The reaction mixture was poured into water, extracted with dichloromethane, washed with aqueous 10% NaOAc, aqueous 4% $NaHCO_3$ and water, dried over Na_2SO_4, and evaporated to dryness. The residue was purified with FCC (5% Et_2O−dichloromethane) and recrystallized from dichloromethane and methanol to give pure **9** as a brown solid (84.6 mg, 70%): VIS (CH_2Cl_2) 703 (relative intensity, 0.92), 652 (0.15), 523 (0.19), 429 nm (1.0); ^{1}H NMR ($CDCl_3$) δ 11.52 (1H, s, 3-CHO), 10.57 (1H, s, 5-H), 9.76 (1H, s, 10-H), 9.08 (1H, s, 20-H), 5.20−5.15, (1H, m, 17-H), 4.69 (1H, q, J = 7 Hz, 18-H), 3.82 (3H, s, 12-CH_3), 3.80 (3H, s, 2-CH_3), 3.75−3.68 (2H, m, 8-CH_2), 3.60 (3H, s, 17^2-CO_2CH_3), 3.32 (3H, s, 7-CH_3), 2.84−2.77, 2.76−2.70, 2.44−2.38, 2.35−2.27 (each 1H, m, 17-CH_2CH_2), 1.90 (3H, d, J = 7 Hz, 18-CH_3), 1.71 (3H, t, J = 7 Hz, 8^1-CH_3), 0.09, −2.17 (each 1H, br-s, NH × 2); HRMS (FAB) *m*/*z* 564.2391 (M^+), calcd for $C_{33}H_{32}N_4O_5$ 564.2373.

Zinc Methyl 15^1-Oxo-pyropheophorbide-*d* (10). To a dichloromethane solution (40 mL) of **9** (84.6 mg, 0.15 mmol) was added a methanol solution (2 mL) saturated with zinc acetate dihydrate, and the mixture was stirred for 2 h under nitrogen. The reaction mixture was poured into water, washed with aqueous 4% $NaHCO_3$ and water, dried over Na_2SO_4, and evaporated to dryness. The residue was recrystallized from dichloromethane and hexane to give pure **10** as a green solid (90.1 mg, 96%): VIS (CH_2Cl_2) 689 (relative intensity, 0.95), 638 (0.12), 543 (0.13), 442 nm (1.0); ^{1}H NMR (1.0% pyridine-d_5−$CDCl_3$) δ 11.43 (1H, s, 3-CHO), 10.55 (1H, s, 5-H), 9.87 (1H, s, 10-H), 8.90 (1H, s, 20-H), 5.11−5.06, (1H, m, 17-H), 4.59 (1H, q, J = 7 Hz, 18-H), 3.87 (3H, s, 12-CH_3), 3.82 (2H, q, J = 7 Hz, 8-CH_2), 3.73 (3H, s, 2-CH_3), 3.57 (3H, s, 17^2-CO_2CH_3), 3.38 (3H, s, 7-CH_3), 2.77−2.70, 2.59−2.52, 2.36−2.29, 2.18−2.10 (each 1H, m, 17-CH_2CH_2), 1.79 (3H, d, J = 7 Hz, 18-CH_3), 1.75 (3H, t, J = 7 Hz, 8^1-CH_3); HRMS (FAB) *m*/*z* 626.1514 (M^+), calcd for $C_{33}H_{30}N_4O_5{}^{64}Zn$ 626.1508.

Zinc Methyl 15^1-Oxo-protopyropheophorbide-*d* (11). Compound **10** (90.1 mg, 0.14 mmol) was dissolved in acetone (50 mL) and pyridine (1 mL), to which an acetone solution (3 mL) of DDQ (76.4 mg, 0.34 mmol) was added and stirred for 10 min. The reaction mixture was poured into aqueous 4% $KHSO_4$ and extracted with chloroform (100 mL) and pyridine (5 mL). The organic layer was washed with aqueous saturated $NaHCO_3$ and water, dried over Na_2SO_4, and evaporated to dryness. The residue was purified by FCC (0.5−1% pyridine−dichloromethane) and recrystallized from 1% pyridine−chloroform and hexane to give pure **11** as a dark green solid (80.5 mg, 90%): VIS (THF) 638 (relative intensity, 0.21), 584 (0.08), 554 (0.08), 443 nm (1.0); ^{1}H NMR (1.0% pyridine-d_5−$CDCl_3$) δ 11.52 (1H, s, 3-CHO), 10.65 (1H, s, 5-H), 9.37 (1H, s, 20-H), 9.20 (1H, s, 10-H), 4.53, (2H, m, 17-CH_2), 3.92 (2H, q, J = 7 Hz, 8-CH_2), 3.87 (3H, s, 2-CH_3), 3.69 (3H, s, 12-CH_3), 3.61 (3H, s, 7-CH_3), 3.56 (3H, s, 17^2-CO_2CH_3), 3.33 (3H, s, 18-CH_3), 2.89 (2H, t, J = 7 Hz, 17^1-CH_2), 1.73 (3H, t, J = 7 Hz, 8^1-CH_3); HRMS (FAB) *m*/*z* 624.1368 (M^+), calcd for $C_{33}H_{28}N_4O_5{}^{64}Zn$ 624.1351.

Zinc Methyl 3-Devinyl-3-hydroxymethyl-15^1-oxo-protopyropheophorbide-*a* (1). Method A: To a dichloromethane (20 mL) and pyridine (1 mL) solution of **11** (28.4 mg, 45 μmol) was added tBuNH$_2$·BH$_3$ (30.0 mg, 0.34 mmol), and the mixture was stirred under nitrogen. After 1 h of stirring, propanal (10 mL) was added, and the reaction mixture was evaporated to dryness. The residue was dissolved in chloroform and washed with water twice, dried over Na_2SO_4, and evaporated to dryness. Normal-phase HPLC separation (Cosmosil 5SLII, 2-propanol/pyridine/1,2-dichloroethane = 2/3/95, 10 × 250 mm, 2.0 mL/min) of the residue gave unchanged **11** (7.8 min), 13-reduced **12** (9.6 min), 3-reduced **1** (12.3 min), and 3,13-reduced **13** (22.5 min) as isolable products. All of the compounds were recrystallized from 1% pyridine−chloroform and hexane, affording pure forms: starting material **11** (4.5 mg, 16%), secondary alcohol **12** (green solid, 8.5 mg, 30%), primary alcohol **1** (green solid, 7.4 mg, 26%) and diol **13** (green solid, 5.4 mg, 19%).

Method B: To a dichloromethane (20 mL) and pyridine (1 mL) solution of **11** (31.5 mg, 50 μmol) was added tBuNH$_2$·BH$_3$ (80.6 mg, 0.93 mmol), and the mixture was stirred under nitrogen. After complete disappearance of the Qy bands at 646 (for **11**) and 625 nm (for **1** and **12**) with a rise of a new Qy band at 607 nm (for **13**), the reaction was quenched by addition of propanal (10 mL). After removal of the solvents in vacuo, the residue was dissolved in chloroform and washed with water twice, dried over Na_2SO_4, and evaporated to dryness, yielding 3^1,13^1-dihydroxylated **13**. The crude product was dissolved in acetone (30 mL) and pyridine (1 mL) and treated with DDQ (29.9 mg, 0.13 mmol), similarly to **10** → **11**. Purification with FCC (1−2% pyridine−dichloromethane) and recrystallization from 1% pyridine−chloroform and hexane gave

pure **1** (24.6 mg, 78% from **11**): VIS (THF) 621 (log ϵ, 4.18), 593 (3.98), 572 (4.07), 553 (3.99), 438 (5.12), 385 nm (4.57); ^{1}H NMR (3.5% pyridine-d_5−$CDCl_3$) δ 10.41 (1H, s, 5-H), 9.88 (1H, s, 20-H), 9.56 (1H, s, 10-H), 6.20 (2H, s, 3-CH_2), 4.52 (2H, m, 17-CH_2), 4.06 (2H, q, J = 7 Hz, 8-CH_2), 3.76 (3H, s, 2-CH_3), 3.71 (3H, br-s, 12-CH_3), 3.68 (3H, s, 7-CH_3), 3.62 (3H, s, 17^2-CO_2CH_3), 3.48 (3H, s, 18-CH_3), 2.99 (2H, br-t, J = 7 Hz, 17^1-CH_2), 1.84 (3H, t, J = 7 Hz, 8^1-CH_3); HRMS (FAB) m/z 626.1513 (M^+), calcd for $C_{33}H_{30}N_4O_5{}^{64}Zn$ 626.1508.

Zinc Methyl 13^1-Deoxo-13^1-hydroxy-15^1-oxo-protopyropheophorbide-*d* (12). VIS (THF) 616 (relative intensity, 0.10), 587 (0.05), 567 (0.05) 545 (0.04), 429 nm (1.0); ^{1}H NMR (1.0% pyridine-d_5−$CDCl_3$) δ 11.36 (1H, s, 3-CHO), 10.56 (1H, s, 5-H), 9.70 (1H, s, 20-H), 9.62 (1H, s, 10-H), 6.42 (1H, s, 13-CH), 4.67−4.58, 4.47−4.40 (each 1H, m, 17-CH_2), 3.93−3.83 (2H, m, 8-CH_2), 3.71 (6H, s, 2-CH_3 + 17^2-CO_2CH_3), 3.64 (3H, s, 12-CH_3), 3.44 (3H, s, 7-CH_3), 3.38 (3H, s, 18-CH_3), 3.24−3.17, 3.16−3.08 (each 1H, m, 17^1-CH_2), 1.79 (3H, t, J = 7 Hz, 8^1-CH_3); HRMS (FAB) m/z 626.1505 (M^+), calcd for $C_{33}H_{30}N_4O_5{}^{64}Zn$ 626.1508.

Zinc Methyl 13^1-Deoxo-3-devinyl-13^1-hydroxy-3-hydroxymethyl-15^1-oxo-protopyropheophorbide-*a* (13). VIS (THF) 600 (relative intensity, 0.16), 588 (sh, 0.11), 555 (0.09), 416 nm (1.0); ^{1}H NMR (3.5% pyridine-d_5−$CDCl_3$) δ 10.28 (1H, s, 5-H), 10.09 (1H, s, 20-H), 9.94 (1H, s, 10-H), 6.57 (1H, s, 13-CH), 6.20 (2H, s, 3-CH_2), 4.78−4.69, 4.62−4.57 (each 1H, m, 17-CH_2), 4.04−3.93 (2H, m, 8-CH_2), 3.74 (3H, s, 12-CH_3), 3.72 (3H, s, 17^2-CO_2CH_3), 3.64 (3H, s, 2-CH_3), 3.56 (3H, s, 18-CH_3), 3.51 (3H, s, 7-CH_3), 3.32−3.25, 3.24−3.15 (each 1H, m, 17^1-CH_2), 1.83 (3H, t, J = 7 Hz, 8^1-CH_3); HRMS (FAB) m/z 628.1676 (M^+), calcd for $C_{33}H_{32}N_4O_5{}^{64}Zn$ 628.1664.

Zinc Methyl 3-Hydroxymethyl-3-devinyl-protopyropheophorbide-*a* (2). The titled compound was prepared according to the reported procedures.[10] VIS (THF) 608 (log ϵ, 4.38), 589 (sh, 3.83), 560 (4.06), 544 (3.86), 524 (3.71), 427 nm (5.35).

Zinc Methyl 13^1-Deoxo-protopyropheophorbide-*a* (15). 13^1-Deoxopyropheophorbide-*a* (**14**,[30] 86.0 mg, 0.16 mmol) was converted to the corresponding zinc porphyrin **15**, similarly to **9** → **10** → **11**. After FCC (dichloromethane), recrystallization from dichloromethane and hexane gave **15** as a red solid (64.5 mg, 67% from **14**): VIS (THF) 573 (relative intensity, 0.03), 543 (0.06), 414 nm (1.0); ^{1}H NMR (1.0% pyridine-d_5−$CDCl_3$) δ 10.06 (2H, s, 5-, 20-H), 9.91 (1H, s, 10-H), 8.41 (1H, dd, J = 18, 11 Hz, 3-CH), 6.38 (1H, dd, J = 18, 1 Hz, 3^1-CH *trans* to 3-CH), 6.10 (1H, dd, J = 11, 1 Hz, 3^1-CH *cis* to 3-CH), 5.43 (2H, m, 13^1-CH_2), 4.36, (2H, m, 17-CH_2), 4.14 (2H, m, 13-CH_2), 4.05 (2H, q, J = 7 Hz, 8-CH_2), 3.80 (3H, s, 17^2-CO_2CH_3), 3.76 (3H, s, 2-CH_3), 3.65 (3H, s, 18-CH_3), 3.63 (3H, s, 12-CH_3), 3.58 (3H, s, 7-CH_3), 3.12 (2H, m, 17^1-CH_2), 1.85 (3H, t, J = 7 Hz, 8^1-CH_3); HRMS (FAB) m/z 594.1971 (M^+), calcd for $C_{34}H_{34}N_4O_2{}^{64}Zn$ 594.1973.

Zinc Methyl 13^1-Deoxo-15^1-oxo-protopyropheophorbide-*a* (16). To a dichloromethane solution (20 mL) of zinc 13^1-deoxoporphyrin **15** (64.5 mg, 0.11 mmol) was added Al_2O_3 (2.4 g), and the mixture was stirred for 10 min under air. The liquid phase became almost colorless, and the Al_2O_3 powder adsorbing any pigments was collected by filtration. The red powder was washed with chloroform−methanol (1:1) solution, and the filtrates were evaporated to dryness, yielding the crude 15^1-hydroxylated product. The residue was dissolved in dichloromethane (20 mL), to which *N*-methylmorpholine *N*-oxide (145.4 mg, 1.2 mmol) and $n$$Pr_4NRuO_4$ (54.6 mg, 0.16 mmol) were added. After 30 min of stirring, the reaction mixture was directly purified by FCC (5−8% Et_2O−dichloromethane) and then recrystallized from dichloromethane and hexane to give pure **16** as a dark green solid (28.8 mg, 44%): VIS (THF) 602 (relative intensity, 0.20), 558 (0.10), 414 nm (1.0); ^{1}H NMR (1.0% pyridined_5−$CDCl_3$) δ 10.12 (1H, s, 5-H), 10.05 (1H, s, 20-H), 9.78 (1H, s, 10-H), 8.30 (1H, dd, J = 18, 11 Hz, 3-CH), 6.31 (1H, dd, J = 18, 1 Hz, 3^1-CH *trans* to 3-CH), 6.10 (1H, dd, J = 11, 1 Hz, 3^1-CH *cis* to 3-CH), 4.70 (2H, s, 13-CH_2), 4.63, (2H, m, 17-CH_2), 3.96 (2H, q, J = 7 Hz, 8-CH_2), 3.73 (3H, s, 17^2-CO_2CH_3), 3.66 (3H, s, 2-CH_3), 3.55$_3$ (3H, s, 18-CH_3), 3.54$_8$ (3H, s, 12-CH_3), 3.51 (3H, s, 7-CH_3), 3.21 (2H, m, 17^1-CH_2), 1.82 (3H, t, J = 7 Hz, 8^1-CH_3); HRMS (FAB) m/z 608.1758 (M^+), calcd for $C_{34}H_{32}N_4O_3{}^{64}Zn$ 608.1766.

Methyl 13^1-Deoxo-15^1-oxo-protopyropheophorbide-*a* (17). To an acetone solution (10 mL) of **16** (28.8 mg, 47 μmol) was added aqueous concentrated HCl (5 mL), and the mixture was stirred for 30 min. The reaction mixture was diluted with water and extracted with chloroform. The organic phase was washed with aqueous 4% $NaHCO_3$ and water, dried over Na_2SO_4, and evaporated to dryness. The residue was purified by FCC (5% Et_2O−dichloromethane) and recrystallized from dichloromethane and hexane to give pure **17** as a green solid (24.6 mg, 95%): VIS (CH_2Cl_2) 637 (relative intensity, 0.18), 584 (0.06), 555 (0.07), 515 (0.08), 408 nm (1.0); ^{1}H NMR ($CDCl_3$) δ 9.69 (1H, s, 5-H), 9.20 (1H, s, 20-H), 9.18 (1H, s, 10-H), 8.03 (1H, dd, J = 18, 11 Hz, 3-CH), 6.21 (1H, d, J = 18 Hz, 3^1-CH *trans* to 3-CH), 6.11 (1H, d, J = 11 Hz, 3^1-CH *cis* to 3-CH), 4.30 (2H, t, J = 7 Hz, 17-CH_2), 4.27 (2H, s, 13-CH_2), 3.86 (2H, q, J = 7 Hz, 8-CH_2), 3.66 (3H, s, 17^2-CO_2CH_3), 3.47 (3H, s, 7-CH_3), 3.36 (3H, s, 2-CH_3), 3.21 (3H, s, 12-CH_3), 3.18 (3H, s, 18-CH_3), 2.89 (2H, t, J = 7 Hz, 17^1-CH_2), 1.73 (3H, t, J = 7 Hz, 8^1-CH_3), −4.24, −5.53 (each 1H, s, NH × 2); MS (FAB) m/z 546 (M^+), calcd for $C_{34}H_{34}N_4O_3$ 546.

Methyl 13^1-Deoxo-15^1-oxo-protopyropheophorbide-*d* (18). Similarly to **8** → **9**, oxidation of **17** (24.6 mg, 45 μmol) gave **18** as a dark green solid (17.1 mg, 69%) after FCC (5−10% Et_2O−dichloromethane) and recrystallization from dichloromethane and hexane: VIS (CH_2Cl_2) 634 (relative intensity, 0.07), 578 (0.08), 528 (0.04), 424 nm (1.0); ^{1}H NMR ($CDCl_3$) δ 11.18 (1H, s, 3-CHO), 10.48 (1H, s, 5-H), 9.27 (1H, s, 10-H), 9.24 (1H, s, 20-H), 4.44, (2H, t, J = 7 Hz, 17-CH_2), 4.39 (2H, br-s, 13-CH_2), 3.92 (2H, q, J = 7 Hz, 8-CH_2), 3.68 (3H, s, 17^2-CO_2CH_3), 3.56 (3H, s, 2-CH_3), 3.52 (3H, s, 7-CH_3), 3.33 (3H, s, 12-CH_3), 3.29 (3H, s, 18-CH_3), 2.97 (2H, t, J = 7 Hz, 17^1-CH_2), 1.77 (3H, t, J = 7 Hz, 8^1-CH_3), −3.75, −4.88 (each 1H, br-s, NH × 2); HRMS (FAB) m/z 548.2420 (M^+), calcd for $C_{33}H_{32}N_4O_4$ 548.2424.

Methyl 13^1-Deoxo-3-devinyl-3-hydroxymethyl-15^1-oxo-protopyropheophorbide-*a* (19). To a dichloromethane (20 mL) solution of 3-formyl-porphyrin **18** (17.1 mg, 31 μmol) was added $t$$BuNH_2$·$BH_3$ (42.5 mg, 0.49 mmol), and the mixture was stirred for 5 h under nitrogen. The reaction mixture was washed with aqueous 2% HCl and water, dried over Na_2SO_4, and evaporated to dryness. The residue was purified with FCC (10% Et_2O–dichloromethane) and recrystallized from chloroform and hexane to give pure **19** as a dark green solid (15.2 mg, 89%): VIS (CH_2Cl_2) 635 (relative intensity, 0.15), 583 (0.04), 556 (0.07), 516 (0.09), 411 nm (1.0); ^{1}H NMR ($CDCl_3$) δ 10.21 (1H, s, 5-H), 9.69 (1H, s, 20-H), 9.59 (1H, s, 10-H), 5.97 (2H, s, 3-CH_2), 4.41 (2H, s, 13-CH_2), 4.37 (2H, t, J = 8 Hz, 17-CH_2), 4.06 (2H, q, J = 7 Hz, 8-CH_2), 3.68 (3H, s, 17^2-CO_2CH_3), 3.66 (3H, s, 7-CH_3), 3.54 (3H, s, 2-CH_3), 3.36 (3H, s, 18-CH_3), 3.34 (3H, s, 12-CH_3), 2.98 (2H, t, J = 8 Hz, 17^1-CH_2), 2.62 (1H, br-s, 3^1-OH), 1.86 (3H, t, J = 7 Hz, 8^1-CH_3), −3.20, −4.52 (each 1H, br-s, NH × 2); HRMS (FAB) m/z 550.2569 (M^+), calcd for $C_{33}H_{34}N_4O_4$ 550.2580.

Zinc Methyl 13^1-Deoxo-3-devinyl-3-hydroxymethyl-15^1-oxo-protpyropheophorbide-*a* (3). Similarly to **9** → **10**, zinc metalation of **19** (15.2 mg, 28 μmol) gave the titled compound **3** as dark green solid (14.9 mg, 88%) after FCC (1−2% methanol−dichloromethane) and recrystallization from chloroform and hexane: VIS (THF) 602 (log ϵ, 4.46), 561 (3.98), 417 nm (5.28); ^{1}H NMR ($CDCl_3$) δ 10.16 (1H, s, 5-H), 10.01 (1H, s, 20-H), 9.77 (1H, s, 10-H), 6.07 (2H, s, 3-CH_2), 4.67 (2H, s, 13-CH_2), 4.59 (2H, t, J = 8 Hz, 17-CH_2), 3.96 (2H, q, J = 7 Hz, 8-CH_2), 3.73 (3H, s, 17^2-CO_2CH_3), 3.63 (3H, s, 2-CH_3), 3.53 (6H, s, 12-, 18-CH_3), 3.51 (3H, s, 7-CH_3), 3.20 (2H, t, J = 8 Hz, 17^1-CH_2), 1.82 (3H, t, J = 7 Hz, 8^1-CH_3); HRMS (FAB) m/z 612.1722 (M^+), calcd for $C_{33}H_{32}N_4O_4{}^{64}Zn$ 612.1715.

Methyl 13^1-Deoxo-pyropheoforbide-*d* (20). Similarly to **8** → **9**, the 3-vinyl group in **14**[30] was converted to the 3-formyl group in **20** (67%).[34] See ref 34 for the spectral data of **20**.

Methyl 3-Devinyl-3-hydroxymethyl-13^1-deoxo-pyropheophorbide-*a* (21). Similarly to **18** → **19**, the 3-formyl group in **20** (28.4 mg, 53 μmol) was reduced to give 3-hydroxymethyl-porphyrin **21** as a green solid (25.4 mg, 89%) after FCC (5% Et_2O−dichloromethane) and recrystallization from dichloromethane and hexane: VIS (CH_2Cl_2) 641 (relative intensity, 0.29), 585 (0.04), 500 (0.10), 395 nm (1.0); ^{1}H NMR ($CDCl_3$) δ 9.91 (1H, s, 5-H), 9.60 (1H, s, 10-H), 8.96 (1H, s, 20-H), 6.07 (2H, s, 3-CH_2), 4.97−4.91, 4.86−4.79 (each 1H, m, 13^1-CH_2), 4.67 (1H, dq, J = 2, 7 Hz, 18-H), 4.50 (1H, m, 17-H), 4.14−4.00 (2H, m, 13-CH_2), 3.87 (2H, q, J = 7 Hz, 8-CH_2), 3.58 (6H, s, 2-CH_3 + 17^2-CO_2CH_3), 3.51 (3H, s, 12-CH_3), 3.44 (3H, s, 7-CH_3), 2.84−2.76, 2.39−2.30 (each 1H, m, 17-CH_2), 2.64−2.57, 2.25−2.18 (each 1H, m, 17^1-CH_2), 2.02 (1H, br-s, 3^1-OH), 1.85 (3H, d, J = 7 Hz, 18-CH_3), 1.77 (3H, t, J = 7 Hz, 8^1-CH_3), −1.71, −3.42 (each 1H, br-s, NH × 2); HRMS (FAB) m/z 538.2945 (M^+), calcd for $C_{33}H_{38}N_4O_3$ 538.2944.

Zinc Methyl 13^1-Deoxo-3-devinyl-3-hydroxymethyl-protopyropheophorbide-*a* (4). Similarly to **9** → **10** → **11**, the chlorin π-system in **21** (25.4 mg, 47 μmol) was converted to the porphyrin π-system, yielding zinc 3-hydroxymethyl-13^1-deoxoporphyrin **4** as a red solid (20.3 mg, 72% from **21**) after FCC (1−2% methanol–dichloromethane) and recrystallization from chloroform and hexane: VIS (THF) 571 (log ϵ, 4.10), 540 (4.18), 409 nm (5.57); ^{1}H NMR (1.0% pyridine-d_5−$CDCl_3$) δ 10.05_3 (1H, s, 5-H), 10.04_8 (1H, s, 20-H), 9.92 (1H, s, 10-H), 6.14 (2H, s, 3-CH_2), 5.43−5.37 (2H, m, 13^1-CH_2), 4.37−4.31 (2H, m, 17-CH_2), 4.15−4.09 (2H, m, 13-CH_2), 4.05 (2H, q, J = 7 Hz, 8-CH_2), 3.80 (3H, s, 17^2-CO_2CH_3), 3.73 (3H, s, 2-CH_3), 3.64 (3H, s, 18-CH_3), 3.62 (3H, s, 12-CH_3), 3.57 (3H, s, 7-CH_3), 3.12 (2H, m, 17^1-CH_2), 1.85 (3H, t, J = 7 Hz, 8^1-CH_3); HRMS (FAB) m/z 598.1919 (M^+), calcd for $C_{33}H_{32}N_4O_4{}^{64}Zn$ 598.1922.

Acknowledgment. We thank Dr. Tomohiro Miyatake of Ryukoku University for his helpful assistance in measurements of HRMS spectra. This work was partially supported by a Grant-in-Aid for Scientific Research (B) (No. 19350088) from JSPS as well as by a Sasakawa Scientific Research Grant from The Japan Science Society.

Supporting Information Available: FT-IR spectra of **1**−**4**, UV−vis and RR spectra of **16**, and 1D and 2D ^{1}H NMR spectra of synthetic compounds. This material is available free of charge via the Internet at http://pubs.acs.org.

JO8014402